Palaeogeography, Palaeoclimatology, Palaeoecology 519 (2019) 1–7

Contents lists available at ScienceDirect

Palaeogeography, Palaeoclimatology, Palaeoecology

journal homepage: www.elsevier.com/locate/palaeo

Preface

The Permian–Triassic transition in the eastern Paleo-Tethys and adjacent regions: Environmental and biotic changes in ocean and on land

1. Introduction

The 20-million-year interval from the late Middle Permian to early Middle Triassic (~260–240 Ma) was a critical period for the evolution of life on Earth. It witnessed two major biocrises: the first at the Guadalupian/Lopingian (Middle/Late Permian) boundary, and the second–the most severe and most protracted biocrisis of the Phanerozoic–at the Permian/Triassic (P–Tr) boundary (Stanley and Yang, 1994; Yin et al., 2007). The P–Tr boundary (PTB) event was followed by multiple secondary episodes of faunal mortality and recovery during the ~5-Myr-long Early Triassic (Bottjer et al., 2008; Chen and Benton, 2012; Song et al., 2013) that were probably linked to episodic global environmental perturbations (Algeo et al., 2011; Retallack et al., 2011; Song et al., 2014). This extended P–Tr transition interval has attracted increasing attention from paleontologists and geologists worldwide. The South China Craton preserves many near-complete and little-altered Upper Permian to Middle Triassic successions representing a range of deep-marine, shallow-marine, and terrestrial facies, which have been intensively studied since the 1980s (Chen and Benton, 2012).

The pace of new findings related to the P–Tr transition coming from studies of South China successions continues to accelerate. Accordingly, we organized a special issue of *Palaeogeography Palaeoclimatology Palaeoecology*, in two volumes, focused on the Paleozoic–Mesozoic transition in South China. The first volume of the special issue (v. 486), which was published in 2017, consisted of 12 papers covering various aspects of the biostratigraphy, paleoecology, sedimentology, geochemistry, and paleoceanography of the transition interval (Chen et al., 2017). The present (second) volume contains a further 18 papers covering the same general topics while advancing our knowledge of these fields with fresh studies from the past two years. The 18 studies of the present volume span the Upper Permian to Triassic of the eastern Paleo-Tethys region (mainly the South China Block) and adjacent areas (Fig. 1; below, blue text indicates studies in this volume). These contributions enhance our understanding of extreme events and organism-environment interactions during this critical period of Earth history.

2. The Permian–Triassic transition in eastern Paleo-Tethys and adjacent regions

2.1. Late Permian biota and environments

A 2nd-order mass extinction has been recognized near the Guadalupian/Lopingian boundary (GLB; =Middle/Late Permian boundary) in South China (Jin, 1993; Stanley and Yang, 1994; Bond et al., 2015), although the significance of this biocrisis has been questioned owing to limited biotic and environmental turnover in most GLB sections (Clapham et al., 2009; Jost et al., 2014), and some studies have claimed that the event was mid-Capitanian in age (Wignall et al., 2009; Bond et al., 2010; Bond and Grasby, 2017).

Reef-community collapse followed by a nektonic extinction was recognized near the GLB in the Penglaitan section of the Laibin area, Guangxi, South China, and linked to contemporaneous oceanic anoxia and volcanism of the Emeishan large igneous province (Zhang et al., 2015; Huang et al., 2019a). It has been estimated that the GLB extinction coincided with a reduction in reef carbonate production of ~90% worldwide (Flügel and Kiessling, 2002). The pattern of reef recovery following the Wuchiapingian collapse remains largely unknown. In this volume, Huang et al. (2019b) document biotic changes in a sponge-reef community of the upper Wuchiapingian Stage in the Tieqiao section, 30 km west of Penglaitan. The Tieqiao reef is the only metazoan buildup in the Wuchiapingian of South China (although metazoan reefs proliferated again during the Changhsingian), and its reemergence in the late Wuchiapingian was much delayed relative to the rebound of level-bottom benthos (i.e., brachiopods) in basal Wuchiapingian strata (Chen et al., 2005; Shen and Shi, 2009). Outside China, metazoan reefs are rare in the Wuchiapingian, and carbonate buildups are mainly bryozoan-microbe reefs (e.g., in the Germanic Basin; Peryt et al., 2016; Raczynski et al., 2017). This reflects a pattern of recovery also seen after other major extinction events (i.e., P–Tr extinction), in which microbial buildups proliferate in the absence of metazoan reefs.

Environmental perturbations prior to the main end-Permian crisis have been recognized only rarely, e.g., in the Canadian Arctic region (Algeo et al., 2012; Schoepfer et al., 2012) and South China (Y.A. Shen et al., 2011; Shen et al., 2012; Lei et al., 2017). In this volume, Tian et al. (2019) document environmental instability in the latest Permian as reflected in biotic and facies variations on some isolated carbonate platforms in the Nanpanjiang Basin. Biodiversity patterns and variations in skeletal composition in three uppermost Permian sections reveal: 1) a faunal shift from non-fusulinid-dominated to fusulinid-dominated communities in the < 1-m interval below the P–Tr extinction horizon, and 2) a “foraminifer gap” coincident with increased influx of detrital siliciclastics prior to the P–Tr crisis. Additional studies are needed to investigate whether the environmental and biotic perturbations predating the main end-Permian crisis were regional or global phenomena.

Accompanying such environmental perturbations during the P–Tr transition may have been large changes in atmospheric pCO_2 levels. Atmospheric CO_2 changes have been estimated in several modeling

https://doi.org/10.1016/j.palaeo.2019.01.011

Available online 12 January 2019

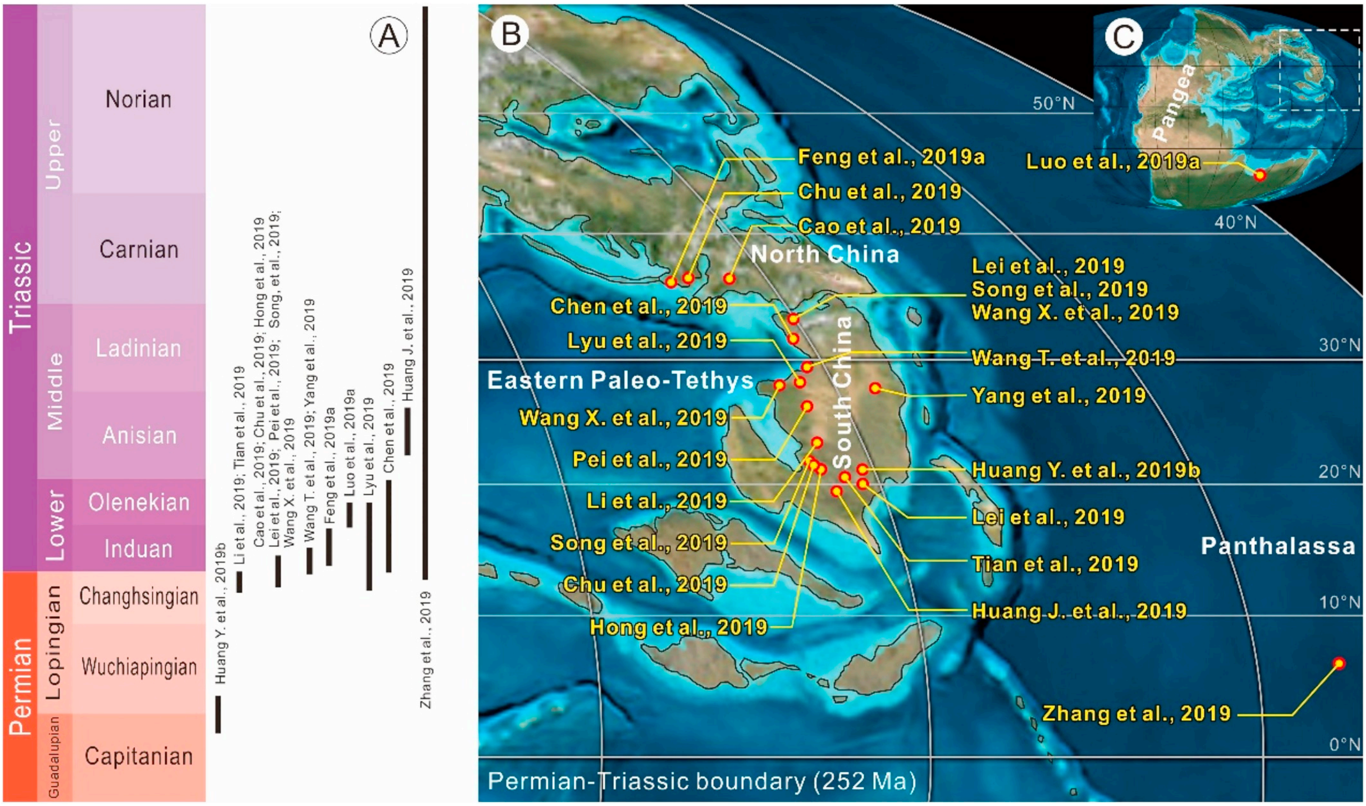

Fig. 1. A, Stratigraphic ranges of 18 studies assembled in this volume. B, Permian–Triassic paleogeographic map of South China and North China cratons (the boxed area in panel C) showing sites of 17 studies in this volume. C, The global paleogeographic inset shows the location of one study in this volume located outside of the main map area (base map after Ron Blakey, deeptimemaps.com). See Reference list for full bibliographic details.

studies (Berner, 2002; Payne and Kump, 2007), but few proxy data are available to ground-truth these model estimates (e.g., Tabor et al., 2004). In this volume, Li et al. (2019) provide the most detailed analysis to date of paleo-atmospheric pCO_2 changes at that time based on well-preserved cuticles from fossil conifers recovered from upper Changhsingian sections in South China. Two modeling approaches, the stomatal ratio method and the mechanistic model (Franks et al., 2014) were applied to generate pCO_2 estimates. These methods yielded pCO_2 estimates of ca. 300–510 ppm and ca. 360–520 ppm, respectively, which are lower than (but somewhat overlapping with) estimates based on coeval paleosols (Retallack, 2001). These paleo-atmospheric CO_2 levels are more consistent with a cool climate rather than cold, glacial conditions during the late Changhsingian.

2.2. *Uppermost Permian to Lower Triassic biochronostratigraphy*

The standard conodont biostratigraphic framework for Upper Permian–Lower Triassic strata of South China has undergone major development over the past decade (e.g., Jiang et al., 2007, 2011; Shen and Mei, 2010; Zhao et al., 2007, 2013a; Z.Q. Chen et al., 2015). The study by Lyu et al. (2019) in this volume contributes to this development, establishing nine uppermost Permian to Lower Triassic conodont zones for the Ganxi and Jianshi areas of western Hubei Province. Although generally conforming to zonation schemes elsewhere in South China, this study recognizes the *Clarkina planata* Zone as a local ecozone reflecting deeper water biofacies during *Hindeodus postparvus* Zone time. It places the P–Tr and Induan–Olenekian (I–O) boundaries at the bases of the *Hindeodus parvus* Zone and *Novispathodus waageni eowaageni* Subzone of the *Nv. waageni* Zone, respectively (cf. Zhao et al., 2007, 2013a; Lyu et al., 2018).

Studies of conodont biostratigraphy in the Panthalassic Ocean region have been severely limited in the past by a paucity of preserved Permian–Triassic strata. The Kamura section of Kyushu Island, Japan, is one of very few shallow-marine facies from the central part of this vast ocean. Previous study of its conodonts (Koike, 1996) and carbon-isotope stratigraphy (Horacek et al., 2009) has been done in a piece-meal fashion, and the conodont work is now outdated. In this volume, Zhang et al. (2019) undertake an integrated conodont and carbon-isotopic study of the Kamura section, recognizing 14 conodont zones from the upper Changhsingian to the upper Norian (Upper Triassic). This section consists of shallow-marine carbonates deposited in an atoll setting in the central Panthalassic Ocean, and gaps spanning the upper Lower Triassic Spathian substage and the upper Middle Triassic Ladinian stage are interpreted to represent eustatic falls and atoll exposure events. This study represents the most detailed biochronological and carbon-isotopic framework for the Triassic of the central Panthalassic region to date, including correlations with coeval biozones and carbon isotopic profiles of the Paleo-Tethys region.

2.3. *Biotic variations during P–Tr transition in marine and terrestrial ecosystems*

Changes in marine biotas during the end-Permian biocrisis and the prolonged ~5-Myr-long Early Triassic recovery interval have been intensively investigated for many years. Some studies have focused on general diversity patterns (Jin et al., 2000), whereas others have focused on specific biotic clades, e.g., bivalves (Posenato et al., 2005; McRoberts, 2010; Hautmann et al., 2011; Tu et al., 2016a), foraminifera (Song et al., 2013), ostracods (Crasquin-Soleau et al., 2007), or conodonts (Orchard, 2007), or specific ecosystem patterns, e.g., reduced tiering (Fraiser and Bottjer, 2005) and faunal miniaturization (the 'Lilliput Effect'; Twitchett, 2007). Changes in microbial communities have also been documented, although most of this work is based on molecular fossils rather than body fossils (Xie et al., 2005, 2010; Cao et al., 2009). Major turnovers are also apparent in terrestrial ecosystems among vertebrates (Smith and Ward, 2001; Benton et al., 2004), land plants (Looy et al., 2001; Hochuli et al., 2010; Yu et al., 2015), and insects (Shcherbakov, 2008). However, changes in some fossil clades and communities with poor fossil records have not received much attention to date, e.g., marine phytoplankton and littoral-zone communities of marginal seas.

Phytoplankton, despite their importance as the base of the marine trophic web, are poorly known from P–Tr transition strata owing to preservational factors. The most commonly preserved types, known as acritarchs, have received some attention (Thomas et al., 2004; Lei et al., 2012; Shen et al., 2013). In this volume, Lei et al. (2019) assess secular changes in acritarch communities in uppermost Permian to Lower Triassic strata of eight South China sections. The recovered acritarchs belong to 25 species in 8 genera and include large-spherical, small-spherical, long-spined, and short-spined forms. Two sharp declines in abundance were identified in the latest Permian *Clarkina meishanensis* Zone and the earliest Triassic *Isarcicella staeschei* Zone, mirroring the two phases of mass extinction among marine invertebrates in South China (Song et al., 2013).

Terrestrial-marine transitional strata are widely present in southwestern South China (e.g., Peng et al., 2005; S.Z. Shen et al., 2011; Yu et al., 2015; Hong et al., 2018), but their faunal assemblages have received limited study to date (Chu et al., 2016). In this volume, Chu et al. (2019) undertake an integrative biostratigraphic study of multiple clades, i.e., conchostracans, plants, insects, and bivalves, with the goal of improving stratigraphic correlations between marine and continental P–Tr transitional beds across China. They show the utility of the *Pteria-Towapteria-Eumorphotis* bivalve assemblage, the *Euestheria gutta*-bearing conchostracan fauna, and the *Euestheria gutta-Magniestheria mangaliensis-Palaeolimnadiopsis vilujensis* conchostracan assemblage for this purpose. In a related study, Song et al. (2019) investigate bivalve assemblages in marginal-marine facies of the Kayitou and Feixianguan formations in five sections in southwestern China. They document 20 species in 13 bivalve genera, assigned to two communities: the *Promyalina–Neoschizodus* and *Pteria* communities. The former is a high-diversity community containing abundant shallow infaunal suspension feeders, whereas the latter is low in diversity and dominated by stationary epifaunal suspension feeders. Conodont correlations with well-studied marine sections in eastern China (i.e., Huangzhishan section; Chen et al., 2009) reveal that the *Promyalina-Neoschizodus* community is of latest Permian age and the *Pteria* community of earliest Triassic age.

Trace fossils have been extensively investigated in P–Tr transition strata (Twitchett and Wignall, 1996; Pruss and Bottjer, 2004; Hofmann et al., 2011, 2015; Chen et al., 2012; Zhao et al., 2015; Feng et al., 2018). Earliest Triassic ichnofossils are exceptionally abundant and diverse in terrestrial-marine transitional settings. In this volume, Feng et al. (2019a) report on a diverse ichnoassemblage from marine interbeds within basal Triassic terrestrial strata in the Houzhougongmiao section of Shaanxi Province, North China. The assemblage contains 17 ichnospecies in 16 ichnogenera and is dominated by epifaunal trace-makers such as shallow-tier ophiuroid traces, scratch marks or trackways of arthropods, and fish swimming traces. This ichnoassemblage indicates that epifauna may have proliferated in marginal marine settings when other biota still suffered post-extinction environmental stresses.

2.4. P–Tr boundary volcanism and terrestrial weathering

K-bentonite beds are a prominent feature of PTB sections in South China, and they provide correlation horizons that are traceable through marine and terrestrial sections across the entire craton (Yang et al., 1991; Yin et al., 1992). These beds have been crucial in yielding zircons for U-Pb dating that have considerably refined the Late Permian–Early Triassic timescale (Bowring et al., 1998; Galfetti et al., 2007; S.Z. Shen et al., 2011; Burgess et al., 2014). Although the nature of these beds has been investigated in some marine sections (e.g., Gao et al., 2013; Deconinck et al., 2014), K-bentonites in terrestrial facies have received little attention. In this volume, Hong et al. (2019) investigate the clay mineralogy and geochemistry of ash beds in two terrestrial sections (Zhejue and Jiucaichong) in eastern Yunnan Province, southwestern China. They infer variations in the intensity of local weathering and volcanic ash sources based on differences in ash-bed elemental and isotopic compositions. These P–Tr bentonites were likely sourced from a continental volcanic arc located on the paleo-southern margin of the South China block.

The felsic volcanic source of the P–Tr ash beds is reinforced by constraints from trace elements and Hf isotopes of zircon grains derived from 21 ash beds of three sections (Shangsi, Jianshi, and Meishan) in South China, as shown by X. Wang et al. (2019) in this volume. Volcanic ash compositions of dacite and rhyolite as well as low Nb/Hf and high Th/Nb ratios of magmatic zircons indicate derivation from silicic, subduction-related igneous activity with little or no basaltic input (cf. Gao et al., 2013). The P–Tr volcanism therefore likely occurred along the convergent southwestern margin of South China as a result of closure of the Paleo-Tethys Ocean. Ash beds near the P–Tr extinction horizon contain zircons with pronounced positive $\varepsilon_{Hf}(t)$ values indicating input of juvenile mantle with limited interaction between magma and crust, implying rapid transit through the crust (cf. Gao et al., 2013).

Mercury (Hg) enrichments have been developed in recent years as a proxy for volcanic inputs to sedimentary successions (Sanei et al., 2012; Sial et al., 2013). Hg anomalies have been reported from many PTB sections globally, implying a source in the Siberian Traps Large Igneous Province (STLIP) (Grasby et al., 2013, 2017; Wang et al., 2018; Shen et al., 2019a). However, Wang et al. (2018) showed that pronounced positive Hg/TOC excursions coincided with ash beds near the PTB in South China that cannot exclude a regional origin, although the same positive excursion does not occur in the ash beds below and above the PTB, suggesting that Hg anomalies may have both a regional and a global component. Moreover, the overlap in time of the felsic volcanism, which was associated with subduction zone magmatism of the Paleo-Tethys, with the STLIP, and the peak in felsic activity at this time likely enhanced the global environmental burden that may have resulted in the P–Tr mass extinction (Chen et al., 2018). Work in progress demonstrates high Hg anomalies in Lower Triassic sections globally from the Griesbachian through the Smithian, suggesting that at least moderate STLIP activity continued until around the Smithian-Spathian boundary, i.e., throughout the first ~1.5 Myr of the Early Triassic (Shen et al., 2019b).

An important consequence of STLIP activity during the Early Triassic and attendant hyperwarming (Sun et al., 2012) was enhanced chemical weathering on land (Retallack, 2005; Sheldon, 2006; Algeo et al., 2011). Recently, new proxies have been used to test changes in weathering fluxes in marine sections, including rare earth elements in conodonts (Zhao et al., 2013b; Li et al., 2017) and lithium (Li) isotopes of the whole-rock samples (Sun et al., 2018). In this volume, Cao et al. (2019) show a major increase in chemical weathering intensity during the P–Tr transition based on chemical index of alteration (CIA) profiles and other weathering indices from two terrestrial sections in North China (Shichuanhe and Yima). All weathering proxies show a positive shift close to the P–Tr extinction horizon, indicating a close relationship between the mass extinction and changes in weathering intensity.

2.5. Marine environmental stresses and microbial proliferation in aftermath of end-Permian mass extinction

Following the end-Permian mass extinction, Early Triassic oceans experienced recurrent episodes of deleterious conditions, marked by high temperatures, anoxia, seawater acidification (Grice et al., 2005; Sun et al., 2012; Clarkson et al., 2015; J. Chen et al., 2015; Huang et al., 2019c). Recent work on carbonate U-isotopes has significantly refined the timing of global-ocean anoxic episodes during the Early Triassic (Lau et al., 2016; Elrick et al., 2017; Zhang et al., 2018). These episodes are thought to have contributed to delays in metazoan recovery, and to have facilitated expansions of microbial communities (Xie et al., 2005, 2010; Chen and Benton, 2012). In this volume, Chen et al. (2019) evaluate the local and global signals of paleoredox conditions in the Lower Triassic of the Chaohu section, eastern China based on redox-sensitive trace elements and molybdenum isotopes. These proxies allow recognition of six intervals of more reducing conditions near the P–Tr and I–O boundaries, in the mid-Smithian, at the Smithian–Spathian boundary, and in the mid- and upper Spathian, matching well with anoxic phases revealed by pyrite framboid analysis of the same section (Huang et al., 2017). The authors conclude that δ^{98}Mo in the Chaohu section is mainly a local redox proxy, although the PTB episode was sufficiently reducing to allow near-quantitative Mo uptake and, thus, preservation of a global seawater δ^{98}Mo signature ($+2.3 \pm 0.2$‰).

Microbialites are widespread in Lower Triassic successions of South China as a result of prolific microbial growth in the disturbed marine environmental conditions following the end-Permian mass extinction (Schubert and Bottjer, 1995; Lehrmann, 1999; Kershaw et al., 2007, 2012; Lehrmann et al., 2015; Fang et al., 2017; Wu et al., 2017). In particular, the P–Tr boundary microbialite (PTBM) has been documented from at least 30 sections in South China (Wu et al., 2017). In this volume, Pei et al. (2019) describe a new PTBM from the Xiajiacao section of western Hubei Province, that is characterized by both "cabbage-like" stromatolites and cm-scale clotted thrombolites. As in other PTBMs (Fang et al., 2017; Wu et al., 2017), *Gakhumella* columns, coccoid- and bacterial clump-like spheroids are abundant at Xiajiacao and thought to have played an important role in microbialite formation. Based on pyrite framboid analysis, these microbial communities are inferred to have thrived under dysoxic conditions. In addition, the microbialite contains few volcanogenic grains (e.g., β-quartz or microspherules), implying that microbial blooms were largely unaffected by contemporaneous volcanism. Also in this volume, T. Wang et al. (2019) present new observations on the PTBM in the Chongyang section of southeastern Hubei Province, documenting an evolution from stratiform stromatolites to tabular thrombolites and then domical thrombolites. Eustatic sea-level changes are inferred to have been the main controlling factor on their growth.

An unusual occurrence of in-situ stromatolitic textures form carbonate nodules within calcareous mudstones of the Tieshikou Formation, just above the PTB in the Tieshikou section, Jiangxi Province, as described by Yang et al. (2019) in this volume. These microbialites are composed of columnar forms and fan-shaped structures. The columnar structures resemble mini-stromatolites in profile, while most branches are patchy or stripe-shaped, with clotted structures in plan view, resembling those of a thrombolite. Fan-shaped cement precipitates consist of multiple crystal fans that have a radiating texture and show distinct growth laminae. The radiating fabrics contain rod-shaped filaments indicative of a microbial origin. Three types of nano-sized structures (intraparticle micropores, fibrous biofilms, and filamentous sheaths) occur in the columns and fans, indicative of bacterial activity during the precipitation of dolomite crystals. The finding of stromatolitic nodules implies that the widely distributed nodular mudstone or argillaceous limestones of earliest Triassic successions in South China may have been deposited in microbe-rich environments in which terrigenous supply was abundant.

Microbially induced sedimentary structures (MISSs) are common forms of biosedimentary structures in shallow-marine siliciclastic environments (Noffke et al., 2003). Wrinkle structures are the most common and best-studied MISSs in marine and terrestrial Lower Triassic strata (Pruss et al., 2004; Mata and Bottjer, 2009; Chu et al., 2015; Tu et al., 2016b; Xu et al., 2017; Feng et al., 2019b). In this volume, Luo et al. (2019a) report on a well-preserved example of wrinkle structures from the Lower Triassic of the Perth Basin, Western Australia, which was a cratonic-interior basin of Gondwana at that time (Chen et al., 2014). These wrinkle structures possess a distinct vertical profile: (1) cross-stratified/laminated sandstone, (2) alternating laminated layers and sandstone layers, (3) laminated layers, and (4) wrinkled layers, in ascending order. Mica flakes in laminations show a preferred alignment parallel to bedding under SEM imaging, suggesting binding and trapping effects by a microbial matground. Moreover, close association of both trace and body fossils with the wrinkle structures in the Perth Basin (Chen et al., 2012) is interpreted to indicate that shelly fauna and trace-making animals may have occupied the matground habitat as a refuge to survive the generally harsh oceanic environmental conditions of the Early Triassic.

2.6. Exceptionally preserved faunas of early Middle Triassic age

Fossil lagerstätten provide key insights into soft-bodied faunas and nearly intact paleo-communities that cannot be gleaned from typical fossil assemblages (Bottjer et al., 2002). The Anisian Luoping Lagerstätte from Luoping County, eastern Yunnan Province, southwestern China, has yielded rich finds of early Middle Triassic marine life, including exceptionally preserved reptiles, fishes, decapods, and arthropods, and abundant ichnofaunas (Luo et al., 2019b), marking the full recovery of marine ecosystems from the P–Tr mass extinction (Chen and Benton, 2012). In this volume, J. Huang et al. (2019) examine conodont assemblages in the Luoping Lagerstätte, reporting on 41 fused conodont clusters (*Nicoraella*) that provide otherwise unobtainable information for reconstruction of the positions of elements in the conodont apparatus. These data provide key insights regarding homologies, evolutionary relationships, function, and feeding patterns among conodont taxa.

3. Concluding remarks

The new findings in this volume, together with those assembled in the first volume of this special issue, represent significant advances on our understanding of biotic-environmental interactions during the Late Permian to Middle Triassic in the eastern Paleo-Tethys and adjacent regions. We are grateful to all contributors, reviewers, and *Palaeo-3* co-editor-in-chief Isabel Montañez for their efforts in completing this thematic special issue.

Editorial work by ZQC is partly supported by four National Natural Science Foundation of China grants (41821001, 41572091, 41772007, 41661134047), and a Hubei Provincial Natural Science Foundation grant (2017CFA019). This is a contribution to IGCP Project 630 "Permian–Triassic climatic and environmental extremes and biotic response".

References

Algeo, T.J., Chen, Z.Q., Fraiser, M.L., Twitchett, R.J., 2011. Terrestrial-marine teleconnections in the collapse and rebuilding of Early Triassic marine ecosystems. Palaeogeogr. Palaeoclimatol. Palaeoecol. 308, 1–11.
Algeo, T.J., Henderson, C.M., Ellwood, B., Rowe, H., Elswick, E., Bates, S., Lyons, T., Hower, J.C., Smith, C., Maynard, B., Hays, L.E., 2012. Evidence for a diachronous Late Permian marine crisis from the Canadian Arctic region. Geol. Soc. Am. Bull. 124, 1424–1448.
Benton, M.J., Tverdokhlebov, V.P., Surkov, M.V., 2004. Ecosystem remodelling among vertebrates at the Permian–Triassic boundary in Russia. Nature 432, 97–100.
Berner, R.A., 2002. Examination of hypotheses for the Permo–Triassic boundary extinction by carbon cycle modeling. Proc. Natl. Acad. Sci. U. S. A. 99, 4172–4177.
Bond, D.P., Grasby, S.E., 2017. On the causes of mass extinctions. Palaeogeogr. Palaeoclimatol. Palaeoecol. 478, 3–29.
Bond, D.P.G., Hilton, J., Wignall, P.B., Ali, J.R., Stevens, L.G., Sun, Y., Lai, X., 2010. The Middle Permian (Capitanian) mass extinction on land and in the oceans. Earth-Sci. Rev. 102, 100–116.
Bond, D.P.G., Wignall, P.B., Joachimski, M.M., Sun, Y., Savov, I., Grasby, S.E., Beauchamp, B., Blomeier, D.P.G., 2015. An abrupt extinction in the Middle Permian (Capitanian) of the Boreal Realm (Spitsbergen) and its link to anoxia and acidification. Geol. Soc. Am. Bull. 127, 1411–1421.
Bottjer, D.J., Etter, W., Hagadorn, J.W., Tang, C.M., 2002. Fossil-Lagerstätten: jewels of the fossil record. In: Bottjer, D.J., Etter, W., Hagadorn, J.W., Tang, C.M. (Eds.),

Exceptional Fossil Preservation: A Unique View on the Evolution of Marine Life. Columbia University Press, New York, pp. 1–10.
Bottjer, D.J., Clapham, M.E., Fraiser, M.L., Powers, C.M., 2008. Understanding mechanisms for the end-Permian mass extinction and the protracted Early Triassic aftermath and recovery. GSA Today 18, 4–10.
Bowring, S.A., Erwin, D.H., Jin, Y.G., Martin, M.W., Davidek, K., Wang, W., 1998. U/Pb zircon geochronology and tempo of the end-Permian mass extinction. Science 280, 1039–1045.
Burgess, S.D., Bowring, S., Shen, S.Z., 2014. High-precision timeline for Earth's most severe extinction. Proc. Natl. Acad. Sci. U. S. A. 111, 3316–3321.
Cao, C., Love, G.D., Hays, L.E., Wang, W., Shen, S., Summons, R.E., 2009. Biogeochemical evidence for euxinic oceans and ecological disturbance presaging the end-Permian mass extinction event. Earth Planet. Sci. Lett. 281, 188–201.
Cao, Y., Song, H.Y., Algeo, T.J., Chu, D.L., Du, Y., Tian, L., Wang, Y.H., Tong, J.N., 2019. Intensified chemical weathering during the Permian–Triassic transition recorded in terrestrial and marine successions. Palaeogeogr. Palaeoclimatol. Palaeoecol (In this volume).
Chen, Z.Q., Benton, M.J., 2012. The timing and pattern of biotic recovery following the end-Permian mass extinction. Nat. Geosci. 5, 375–383.
Chen, Z.Q., Campi, M.J., Shi, G.R., Kaiho, K., 2005. Post-extinction brachiopod faunas from the Late Permian Wuchiapingian coal series of South China. Acta Palaeontol. Pol. 50, 343–363.
Chen, Z.Q., Tong, J., Zhang, K., Yang, H., Liao, Z., Song, H., Chen, J., 2009. Environmental and biotic turnover across the Permian–Triassic boundary on a shallow carbonate platform in western Zhejiang, South China. Aust. J. Earth Sci. 56, 775–797.
Chen, Z.Q., Fraiser, M.L., Bolton, C., 2012. Early Triassic trace fossils from Gondwana interior sea: implication for ecosystem recovery following the end-Permian mass extinction in south high-latitude region. Gondwana Res. 22, 238–255.
Chen, Z.Q., Wang, Y.B., Kershaw, S., Luo, M., Yang, H., Zhao, L., Fang, Y., Chen, J., Li, Y., Zhang, L., 2014. Early Triassic stromatolites in a siliciclastic nearshore setting in northern Perth Basin, Western Australia: geobiologic features and implications for post-extinction microbial proliferation. Glob. Planet. Chang. 121, 89–100.
Chen, J., Algeo, T.J., Zhao, L., Chen, Z.Q., Cao, L., Zhang, L., Li, Y., 2015a. Diagenetic uptake of rare earth elements by bioapatite, with an example from Lower Triassic conodonts of South China. Earth-Sci. Rev. 149, 181–202.
Chen, Z.Q., Yang, H., Luo, M., Benton, M.J., Kaiho, K., Zhao, L., Huang, Y., Zhang, K., Fang, Y., Jiang, H., Qiu, H., Li, Y., Tu, C., Shi, L., Zhang, L., Feng, X., Chen, L., 2015b. Complete biotic and sedimentary records of the Permian–Triassic transition from Meishan section, South China: ecologically assessing mass extinction and its aftermath. Earth-Sci. Rev. 149, 67–107.
Chen, Z.Q., Algeo, T.J., Sun, Y., Schoepfer, S., 2017. The Paleozoic-Mesozoic transition in South China: oceanic environments and life from Late Permian to Late Triassic. Palaeogeogr. Palaeoclimatol. Palaeoecol. 486, 1–5.
Chen, Z.Q., Zhao, L., Wang, X., Luo, M., Guo, Z., 2018. Great Paleozoic-Mesozoic biotic turnings and paleontological education in China: a tribute to the achievements of Professor Zunyi Yang. J. Earth Sci. 29, 721–732.
Chen, J., Zhao, L., Algeo, T.J., Zhou, L., Zhang, L., Qiu, H., 2019. Evaluation of paleomarine redox conditions using Mo-isotope data in low [Mo] sediments: a case study from the Lower Triassic of South China. Palaeogeogr. Palaeoclimatol. Palaeoecol (In this volume).
Chu, D., Tong, J., Song, H.J., Benton, M.J., Bottjer, D.J., Song, H.Y., Tian, L., 2015. Early Triassic wrinkle structures on land: stressed environments and oases for life. Sci. Rep. 5, 10109e.
Chu, D., Yu, J., Tong, J., Benton, M.J., Song, H., Huang, Y., Song, T., Tian, L., 2016. Biostratigraphic correlation and mass extinction during the Permian–Triassic transition in terrestrial-marine siliciclastic settings of South China. Glob. Planet. Chang. 146, 67–88.
Chu, D., Tong, J., Benton, M.J., Yu, J., Huang, Y., 2019. Mixed continental-marine biotas following the Permian–Triassic mass extinction in South and North China. Palaeogeogr. Palaeoclimatol. Palaeoecol (In this volume).
Clapham, M.E., Shen, S., Bottjer, D.J., 2009. The double mass extinction revisited: reassessing the severity, selectivity, and causes of the end-Guadalupian biotic crisis (Late Permian). Paleobiology 35, 32–50.
Clarkson, M.O., Kasemann, S.A., Wood, R.A., Lenton, T.M., Daines, S.J., Richoz, S., Ohnemueller, F., Meixner, A., Poulton, S.W., Tipper, E.T., 2015. Ocean acidification and the Permo–Triassic mass extinction. Science 348, 229–232.
Crasquin-Soleau, S., Galfetti, T., Bucher, H., Kershaw, S., Feng, Q., 2007. Ostracod recovery in the aftermath of the Permian–Triassic crisis: Palaeozoic–Mesozoic turnover. In: Matzke-Karasz, R., Martens, K., Schudack, M. (Eds.), Ostracodology—Linking Bio- and Geosciences. Springer, Dordrecht, pp. 13–27.
Deconinck, J.F., Crasquin, S., Bruneau, L., Pellenard, P., Baudin, F., Feng, Q., 2014. Diagenesis of clay minerals and K-bentonites in Late Permian/Early Triassic sediments of the Sichuan Basin (Chaotian section, Central China). J. Asian Earth Sci. 81, 28–37.
Elrick, M., Polyak, V., Algeo, T.J., Romaniello, S., Asmerom, Y., Herrmann, A.D., Anbar, A.D., Zhao, L., Chen, Z.Q., 2017. Global-ocean redox variation during the middle-late Permian through Early Triassic based on uranium isotope and Th/U trends of marine carbonates. Geology 45, 163–166.
Fang, Y., Chen, Z.Q., Kershaw, S., Yang, H., Luo, M., 2017. Permian–Triassic boundary microbialites at Zuodeng section, Guangxi Province, South China: geobiology and palaeoceanographic implications. Glob. Planet. Chang. 152, 115–128.
Feng, X., Chen, Z.Q., Bottjer, D.J., Fraiser, M.L., Xu, Y., Luo, M., 2018. Additional records of ichnogenus *Rhizocorallium* from the Lower and Middle Triassic, South China: implications for biotic recovery after the end-Permian mass extinction. Geol. Soc. Am. Bull. 130, 1197–1215.
Feng, X., Chen, Z.Q., Benton, M.J., Wu, S.Q., Bottjer, D.J., Thompson, J.R., 2019a. A diverse trackway-dominated marine ichnoassemblage from the Lower Triassic in the northern Paleotethys: Ichnology and implications for biotic recovery. Palaeogeogr. Palaeoclimatol. Palaeoecol (In this volume).
Feng, X., Chen, Z.Q., Bottjer, D.J., Wu, S., Zhao, L., Xu, Y., Shi, G.R., Huang, Y., Fang, Y., Tu, C., 2019b. Unusual shallow marine matground-adapted benthic biofacies from the Lower Triassic of the northern Paleotethys: implications for biotic recovery following the end-Permian mass extinction. Earth-Sci. Rev. https://doi.org/10.1016/j.earscirev.2018.07.012. (in press).
Flügel, E., Kiessling, W., 2002. Patterns of Phanerozoic reef crisis. In: Kiessling, W., Flügel, E., Golonka, J. (Eds.), Phanerozoic Reef Patterns. SEPM Spec. Publ. 72pp. 339–390.
Fraiser, M.L., Bottjer, D.J., 2005. Restructuring in benthic level-bottom shallow marine communities due to prolonged environmental stress following the end-Permian mass extinction. C.R. Palevol 4, 583–591.
Franks, P.J., Royer, D.L., Beerling, D.J., Van de Water, P.K., Cantrill, D.J., Barbour, M.M., Berry, J.A., 2014. New constraints on atmospheric CO_2 concentration for the Phanerozoic. Geophys. Res. Lett. 41, 4685–4694.
Galfetti, T., Bucher, H., Ovtcharova, M., Schaltegger, U., Brayard, A., Brühwiler, T., Goudemand, N., Weissert, H., Hochuli, P.A., Cordey, F., Guodun, K., 2007. Timing of the Early Triassic carbon cycle perturbations inferred from new U-Pb ages and ammonoid biochronozones. Earth Planet. Sci. Lett. 258, 593–604.
Gao, Q., Zhang, N., Xia, W., Feng, Q., Chen, Z.Q., Zheng, J., Griffin, W.L., O'Reilly, S.Y., Pearson, N.J., Wang, G., Wu, S., Zhong, W., Sun, X., 2013. Origin of volcanic ash beds across the Permian–Triassic boundary, Daxiakou, South China: petrology and U-Pb age, trace elements and Hf-isotope composition of zircon. Chem. Geol. 360-361, 41–53.
Grasby, S.E., Sanei, H., Beauchamp, B., Chen, Z., 2013. Mercury deposition through the Permo–Triassic biotic crisis. Chem. Geol. 351, 209–216.
Grasby, S.E., Shen, W., Yin, R., Gleason, J., Blum, J., Lepak, R., Hurley, J., Beauchamp, B., 2017. Isotopic signatures of mercury contamination in latest Permian oceans. Geology 45, 55–58.
Grice, K., Cao, C., Love, G.D., Böttcher, M.E., Twitchett, R.J., Grosjean, E., Summons, R.E., Turgeon, S.C., Dunning, W., Jin, Y., 2005. Photic zone euxinia during the Permian–Triassic superanoxic event. Science 307, 706–709.
Hautmann, M., Bucher, H., Brühwiler, T., Goudemand, N., Kaim, A., Nützel, A., 2011. An unusually diverse mollusc fauna from the earliest Triassic of South China and its implications for benthic recovery after the end-Permian biotic crisis. Geobios 44, 71–85.
Hochuli, P.A., Vigran, J.O., Hermann, E., Bucher, H., 2010. Multiple climatic changes around the Permian–Triassic boundary event revealed by an expanded palynological record from mid-Norway. Geol. Soc. Am. Bull. 122, 884–896.
Hofmann, R., Goudemand, N., Wasmer, M., Bucher, H., Hautmann, M., 2011. New trace fossil evidence for an early recovery signal in the aftermath of the end-Permian mass extinction. Palaeogeogr. Palaeoclimatol. Palaeoecol. 310, 216–226.
Hofmann, R., Buatois, L.A., MacNaughton, R.B., Mangano, M.G., 2015. Loss of the sedimentary mixed layer as a result of the end-Permian extinction. Palaeogeogr. Palaeoclimatol. Palaeoecol. 428, 1–11.
Hong, H., Algeo, T.J., Fang, Q., Zhao, L., Kaipeng, J., Yin, K., Wang, C., Shi, C., 2018. Facies dependence of the mineralogy and geochemistry of altered volcanic ash beds: an example from Permian–Triassic transition strata in southwestern China. Earth-Sci. Rev (in press).
Hong, H., Zhao, L., Fang, Q., Algeo, T.J., Wang, C., Yu, J., Gong, N., Yin, K., Ji, K., 2019. Volcanic sources and diagenetic alteration of Permian–Triassic boundary K-bentonites in Guizhou Province, South China. Palaeogeogr. Palaeoclimatol. Palaeoecol (In this volume).
Horacek, M., Koike, T., Richoz, S., 2009. Lower Triassic $\delta^{13}C$ isotope curve from shallow-marine carbonates in Japan, Panthalassa realm: confirmation of the Tethys $\delta^{13}C$ curve. J. Asian Earth Sci. 36, 481–490.
Huang, Y., Chen, Z.Q., Wignall, P.B., Zhao, L., 2017. Latest Permian to Middle Triassic redox condition variations in ramp settings, South China: pyrite framboid evidence. Geol. Soc. Am. Bull. 129, 229–243.
Huang, J., Hu, S., Zhang, Q., Donoghuee, P.C.J., Benton, M.J., Zhou, C., Martínez-Pérez, C., Wen, W., Xie, T., Chen, Z.Q., Luo, M., Yao, H., Zhang, K., 2019. Gondolelloid multielement conodont apparatus (*Nicoraella*) from the Middle Triassic of Yunnan Province, southwestern China. Palaeogeogr. Palaeoclimatol. Palaeoecol (In this volume).
Huang, Y., Chen, Z.Q., Wignall, P.B., Grasby, S.E., Zhao, L., Wang, X., Kaiho, K., 2019a. Biotic responses to volatile volcanism and environmental stresses over the Guadalupian–Lopingian (Permian) transition. Geology. https://doi.org/10.1130/G45283.1. (in press).
Huang, Y., Chen, Z.Q., Zhao, L., Stanley Jr., G.D., Yan, J., Pei, Y., Wang, W., Huang, J., 2019b. Restoration of reef ecosystems following the Guadalupian–Lopingian boundary mass extinction: evidence from the Laibin area, South China. Palaeogeogr. Palaeoclimatol. Palaeoecol (In this volume).
Huang, Y., Chen, Z.Q., Algeo, T.J., Zhao, L., Baud, A., Bhate, G.M., Zhang, L., Guo, Z., 2019c. Two-stage marine anoxia and biotic response during the Permian–Triassic transition in Kashmir, northern India: pyrite framboid evidence. Glob. Planet. Chang. 172, 124–139.
Jiang, H., Lai, X., Luo, G., Aldridge, R., Zhang, K., Wignall, P., 2007. Restudy of conodont zonation and evolution across the P/T boundary at Meishan section, Changxing, Zhejiang, China. Glob. Planet. Chang. 55, 39–55.
Jiang, H., Lai, X., Yan, C., Aldridge, R.J., Wignall, P., Sun, Y., 2011. Revised conodont zonation and conodont evolution across the Permian–Triassic boundary at the Shangsi section, Guangyuan, Sichuan, South China. Glob. Planet. Chang. 77, 103–115.

Jin, Y.G., 1993. Pre-Lopingian benthos crisis. In: Comptes Rendus XII ICC-P. 2. pp. 269–278.
Jin, Y.G., Wang, Y., Wang, W., Shang, Q.H., Cao, C.Q., Erwin, D.H., 2000. Pattern of marine mass extinction near the Permian–Triassic boundary in South China. Science 289, 432–436.
Jost, A.B., Mundil, R., He, B., Brown, S.T., Altiner, D., Sun, Y., DePaolo, D., Payne, J.L., 2014. Constraining the cause of the end-Guadalupian extinction with coupled records of carbon and calcium isotopes. Earth Planet. Sci. Lett. 396, 201–212.
Kershaw, S., Li, Y., Crasquin-Soleau, S., Feng, Q., Mu, X., Collin, P.Y., Reynolds, A., Guo, L., 2007. Earliest Triassic microbialites in the South China block and other areas: controls on their growth and distribution. Facies 53, 409–425.
Kershaw, S., Crasquin, S., Li, Y., Collin, P.Y., Forel, M.B., Mu, X., Baud, A., Wang, Y., Xie, S., Maurer, F., Guo, L., 2012. Microbialites and global environmental change across the Permian–Triassic boundary: a synthesis. Geobiology 10, 25–47.
Koike, T., 1996. The first occurrence of Griesbachian conodonts in Japan. Trans. Proc. Palaeontol. Soc. Jpn. New Ser. 181, 337–346.
Lau, K.V., Maher, K., Altiner, D., Kelley, B.M., Kump, L.R., Lehrmann, D.J., Silva-Tamayo, J.C., Weaver, K.L., Yu, M., Payne, J.L., 2016. Marine anoxia and delayed Earth system recovery after the end-Permian extinction. Proc. Natl. Acad. Sci. U. S. A. 113, 2360–2365.
Lehrmann, D.J., 1999. Early Triassic calcimicrobial mounds and biostromes of the Nanpanjiang basin, south China. Geology 27, 359–362.
Lehrmann, D.J., Bentz, J.M., Wood, T., Goers, A., Dhillon, R., Akin, S., Li, X., Payne, J.L., Kelley, B.M., Meyer, K.M., Schaal, E.K., 2015. Environmental controls on the genesis of marine microbialites and dissolution surface associated with the end-Permian mass extinction: new sections and observations from the Nanpanjiang Basin, South China. Palaios 30, 529–552.
Lei, Y., Servais, T., Feng, Q., He, W., 2012. The spatial (nearshore–offshore) distribution of latest Permian phytoplankton from the Yangtze Block, South China. Palaeogeogr. Palaeoclimatol. Palaeoecol. 363, 151–162.
Lei, L., Shen, J., Li, C., Algeo, T.J., Chen, Z.Q., Feng, Q., Cheng, M., Jin, C., Huang, J., 2017. Controls on regional marine redox evolution during the Permian–Triassic transition in South China. Palaeogeogr. Palaeoclimatol. Palaeoecol. 486, 17–32.
Lei, Y., Shen, J., Algeo, T.J., Servaise, T., Feng, Q., Yu, J., 2019. Phytoplankton (acritarch) community changes during the Permian–Triassic transition in South China. Palaeogeogr. Palaeoclimatol. Palaeoecol (In this volume).
Li, Y., Zhao, L., Chen, Z.Q., Algeo, T.J., Cao, L., Wang, X., 2017. Oceanic environmental changes on a shallow carbonate platform (Yangou, Jiangxi, South China) during the Permian–Triassic transition: evidence from rare earth elements of conodont bioapatite. Palaeogeogr. Palaeoclimatol. Palaeoecol. 486, 6–16.
Li, H., Yu, J.X., McElwain, J.C., Yiotis, C., Chen, Z.Q., 2019. Reconstruction of atmospheric CO_2 concentration during the late Changhsingian based on fossil conifers from the Dalong Formation in South China. Palaeogeogr. Palaeoclimatol. Palaeoecol (In this volume).
Looy, C.V., Twitchett, R.J., Dilcher, D.L., Van Konijnenburg-Van Cittert, J.H., Visscher, H., 2001. Life in the end-Permian dead zone. Proc. Natl. Acad. Sci. U. S. A. 98, 7879–7883.
Luo, M., Chen, Z.Q., Shi, G.R., Feng, X., Yang, H., Fang, Y., Li, Y., 2019a. Microbially induced sedimentary structures (MISSs) from the Lower Triassic Kockatea Formation, northern Perth Basin, Western Australia: palaeoenvironmental implications. Palaeogeogr. Palaeoclimatol. Palaeoecol (In this volume).
Luo, M., Shi, G.R., Hu, S., Benton, M.J., Chen, Z.Q., Huang, J., Zhang, Q., Zhou, C., Wen, W., 2019b. Early Middle Triassic trace fossils from the Luoping Biota, southwestern China: evidence of recovery from mass extinction. Palaeogeogr. Palaeoclimatol. Palaeoecol. 515, 6–22.
Lyu, Z., Orchard, M.J., Chen, Z.Q., Zhao, L., Zhang, L., Zhang, X., 2018. A taxonomic reassessment of the *Novispathodus waageni* group and its role in defining the base of the Olenekian (Lower Triassic). J. Earth Sci. 29, 824–836.
Lyu, Z., Orchard, M.J., Chen, Z.Q., Wang, X., Zhao, L., Han, C., 2019. Uppermost Permian to Lower Triassic conodont successions from the Enshi area, western Hubei Province, South China. Palaeogeogr. Palaeoclimatol. Palaeoecol (In this volume).
Mata, S.A., Bottjer, D.J., 2009. Development of Lower Triassic wrinkle structures: implications for the search for life on other planets. Astrobiology 9, 895–906.
McRoberts, C.A., 2010. Biochronology of Triassic bivalves. In: Lucas, S.G. (Ed.), The Triassic Timescale. Geol. Soc. London Spec. Publ 334. pp. 201–219.
Noffke, N., Gerdes, G., Klenke, T., 2003. Benthic cyanobacteria and their influence on the sedimentary dynamics of peritidal depositional systems (siliciclastic, evaporitic salty, and evaporitic carbonatic). Earth-Sci. Rev. 12, 1–14.
Orchard, M.J., 2007. Conodont diversity and evolution through the latest Permian and Early Triassic upheavals. Palaeogeogr. Palaeoclimatol. Palaeoecol. 252, 93–117.
Payne, J.L., Kump, L.R., 2007. Evidence for recurrent Early Triassic massive volcanism from quantitative interpretation of carbon isotope fluctuations. Earth Planet. Sci. Lett. 256, 264–277.
Pei, Y., Chen, Z.Q., Fang, Y., Kershaw, S., Wu, S., Luo, M., 2019. Volcanism, redox conditions, and microbialite growth linked with the end-Permian mass extinction: evidence from the Xiajiacao section (western Hubei Province), South China. Palaeogeogr. Palaeoclimatol. Palaeoecol (In this volume).
Peng, Y., Zhang, S., Yu, T., Yang, F., Gao, Y., Shi, G.R., 2005. High-resolution terrestrial Permian–Triassic eventostratigraphic boundary in western Guizhou and eastern Yunnan, southwestern China. Palaeogeogr. Palaeoclimatol. Palaeoecol. 215, 285–295.
Peryt, T.M., Raczyński, P., Peryt, D., Chłódek, K., Mikołajewski, Z., 2016. Sedimentary history and biota of the Zechstein limestone (Permian, Wuchiapingian) of the Jabłonna reef in Western Poland. Ann. Soc. Geol. Pol. 86, 379–413.
Posenato, R., Pelikan, P., Hips, K., 2005. Bivalves and brachiopods near the Permian-Triassic boundary from the Bükk Mountains (Balvany-North section, Northern Hungary). Riv. Ital. Paleontol. Stratigr. 111, 215–232.
Pruss, S.B., Bottjer, D.J., 2004. Early Triassic trace fossils of the western United States and their implications for prolonged environmental stress from the end-Permian mass extinction. Palaios 19, 551–564.
Pruss, S.B., Fraiser, M., Bottjer, D.J., 2004. Proliferation of Early Triassic wrinkle structures: implications for environmental stress following the end-Permian mass extinction. Geology 32, 461–464.
Raczynski, P., Peryt, T.M., Strobel, W., 2017. Sedimentary and environmental history of the Late Permian Bonikowo Reef (Zechstein Limestone, Wuchiapingian), western Poland. J. Palaeogeogr. 6, 183–205.
Retallack, G.J., 2001. A 300-million-year record of atmospheric carbon dioxide from fossil plant cuticles. Nature 411, 287–290.
Retallack, G.J., 2005. Earliest Triassic claystone breccias and soil-erosion crisis. J. Sediment. Res. 75, 679–695.
Retallack, G.J., Sheldon, N.D., Carr, P.F., Fanning, M., Thompson, C.A., Williams, M.L., Jones, B.G., Hutton, A., 2011. Multiple Early Triassic greenhouse crises impeded recovery from Late Permian mass extinction. Palaeogeogr. Palaeoclimatol. Palaeoecol. 308, 233–251.
Sanei, H., Grasby, S.E., Beauchamp, B., 2012. Latest Permian mercury anomalies. Geology 40, 63–66.
Schoepfer, S.D., Henderson, C.M., Garrison, G.H., Ward, P.D., 2012. Cessation of a productive coastal upwelling system in the Panthalassic Ocean at the Permian–Triassic boundary. Palaeogeogr. Palaeoclimatol. Palaeoecol. 313, 181–188.
Schubert, J.K., Bottjer, D.J., 1995. Aftermath of the Permian-Triassic mass extinction event: Paleoecology of Lower Triassic carbonates in the western USA. Palaeogeogr. Palaeoclimatol. Palaeoecol. 116, 1–39.
Shcherbakov, D.E., 2008. On Permian and Triassic insect faunas in relation to biogeography and the Permian–Triassic crisis. Paleontol. J. 42, 15–31.
Sheldon, N.D., 2006. Abrupt chemical weathering increase across the Permian–Triassic boundary. Palaeogeogr. Palaeoclimatol. Palaeoecol. 231, 315–321.
Shen, S.Z., Mei, S.L., 2010. Lopingian (Late Permian) high-resolution conodont biostratigraphy in Iran with comparison to South China zonation. Geol. J. 45, 135–161.
Shen, S.Z., Shi, G.R., 2009. Latest Guadalupian brachiopods from the Guadalupian/Lopingian boundary GSSP section at Penglaitan in Laibin, Guangxi, South China and implications for the timing of the pre-Lopingian crisis. Palaeoworld 18, 152–161.
Shen, S.Z., Crowley, J.L., Wang, Y., Bowring, S.A., Erwin, D.H., Sadler, P.M., Cao, C.Q., Rothman, D.H., Henderson, C.M., Ramezani, J., Zhang, H., 2011a. Calibrating the end-Permian mass extinction. Science 334, 1367–1372.
Shen, Y.A., Farquhar, J., Zhang, H., Masterson, A., Zhang, T., Wing, B., 2011b. Multiple S-isotopic evidence for episodic shoaling of anoxic water during Late Permian mass extinction. Nat. Commun. 2, 210e.
Shen, J., Algeo, T.J., Zhou, L., Feng, Q., Yu, J., Ellwood, B., 2012. Volcanic perturbations of the marine environment in South China preceding the latest Permian mass extinction and their biotic effects. Geobiology 10, 82–103.
Shen, J., Lei, Y., Algeo, T.J., Feng, Q., Servais, T., Yu, J., Zhou, L., 2013. Volcanic effects on microplankton during the Permian–Triassic transition (Shangsi and Xinmin, South China). Palaios 28, 552–567.
Shen, J., Chen, J., Algeo, T.J., Yuan, S., Feng, Q., Yu, J., Zhou, L., O'Connell, B., Planavsky, N.J., 2019a. Evidence for a prolonged Permian–Triassic extinction interval from global marine mercury records. Nat. Commun (in press).
Shen, J., Algeo, T.J., Planavsky, N.J., Yu, J., Feng, Q., Song, H.J., Song, H.Y., Rowe, H.D., Zhou, L., Chen, J., 2019b. Mercury enrichments provide evidence of Early Triassic volcanism following the end-Permian mass extinction. Earth-Sci. Rev (in press).
Sial, A.N., Lacerda, L.D., Ferreira, V.P., Frei, R., Marquillas, R.A., Barbosa, J.A., Gaucher, C., Windmöller, C.C., Pereira, N.S., 2013. Mercury as a proxy for volcanic activity during extreme environmental turnover: the Cretaceous–Paleogene transition. Palaeogeogr. Palaeoclimatol. Palaeoecol. 387, 153–164.
Smith, R.M., Ward, P.D., 2001. Pattern of vertebrate extinctions across an event bed at the Permian–Triassic boundary in the Karoo Basin of South Africa. Geology 29, 1147–1150.
Song, H.J., Wignall, P.B., Tong, J., Yin, H.F., 2013. Two pulses of extinction during the Permian–Triassic crisis. Nat. Geosci. 6, 52–56.
Song, H.Y., Tong, J., Algeo, T.J., Song, H.J., Qiu, H., Zhu, Y., Tian, L., Bates, S., Lyons, T.W., Luo, G., Kump, L.R., 2014. Early Triassic seawater sulfate drawdown. Geochim. Cosmochim. Acta 128, 95–113.
Song, T., Tong, J., Tian, L., Chu, D., Huang, Y., 2019. Taxonomic and ecological variations of Permian–Triassic transitional bivalve communities from the littoral clastic facies in southwestern China. Palaeogeogr. Palaeoclimatol. Palaeoecol (In this volume).
Stanley, S., Yang, X., 1994. A double mass extinction at the end of the Paleozoic era. Science 266, 1340–1344.
Sun, Y., Joachimski, M.M., Wignall, P.B., Yan, C., Chen, Y., Jiang, H., Wang, L., Lai, X., 2012. Lethally hot temperatures during the Early Triassic greenhouse. Science 338, 366–370.
Sun, H., Xiao, Y.L., Gao, Y., Zhang, G., Casey, J.F., Shen, Y.A., 2018. Rapid enhancement of chemical weathering recorded by extremely light seawater lithium isotopes at the Permian–Triassic boundary. Proc. Natl. Acad. Sci. U. S. A. 115, 3782–3787.
Tabor, N.J., Yapp, C.J., Montañez, I.P., 2004. Goethite, calcite, and organic matter from Permian and Triassic soils: carbon isotopes and CO_2 concentrations. Geochim. Cosmochim. Acta 68, 1503–1517.
Thomas, B.M., Willink, R.J., Grice, K., Twitchett, R.J., Purcell, R.R., Archbold, N.W., George, A.D., Tye, S., Alexander, R., Foster, C.B., Barber, C.J., 2004. Unique marine Permian–Triassic boundary section from Western Australia. Aust. J. Earth Sci. 51, 423–430.
Tian, L., Tong, J., Xiao, Y., Benton, M.J., Song, H.Y., Song, H.J., Liang, L., Wu, K., Chu, D., Algeo, T.J., 2019. Environmental instability prior to end-Permian mass extinction reflected in biotic and facies changes on shallow carbonate platforms of the

Nanpanjiang Basin (South China). Palaeogeogr. Palaeoclimatol. Palaeoecol (In this volume).
Tu, C., Chen, Z.Q., Harper, D.A., 2016a. Permian–Triassic evolution of the Bivalvia: extinction-recovery patterns linked to ecologic and taxonomic selectivity. Palaeogeogr. Palaeoclimatol. Palaeoecol. 459, 53–62.
Tu, C., Chen, Z.Q., Retallack, G.J., Huang, Y., Fang, Y., 2016b. Proliferation of MISS-related microbial mats following the end-Permian mass extinction in terrestrial ecosystems: evidence from the Lower Triassic of the Yiyang area, Henan Province, North China. Sediment. Geol. 333, 50–69.
Twitchett, R.J., 2007. The Lilliput effect in the aftermath of the end-Permian extinction event. Palaeogeogr. Palaeoclimatol. Palaeoecol. 252, 132–144.
Twitchett, R.J., Wignall, P.B., 1996. Trace fossils and the aftermath of the Permo-Triassic mass extinction: evidence from northern Italy. Palaeogeogr. Palaeoclimatol. Palaeoecol. 124, 137–151.
Wang, X., Cawood, P., Zhao, H., Zhao, L., Grasby, S.E., Chen, Z.Q., Wignall, P.B., Lyu, Z., Han, C., 2018. Mercury anomalies across the end Permian mass extinction in South China from shallow and deep-water depositional environments. Earth Planet. Sci. Lett. 496, 159–167.
Wang, T., Burne, R.V., Yuan, A., Wang, Y., Yi, Z., 2019a. The evolution of microbialite forms during the Early Triassic transgression: a case study in Chongyang of Hubei Province, South China. Palaeogeogr. Palaeoclimatol. Palaeoecol (In this volume).
Wang, X., Cawood, P.A., Zhao, L., Chen, Z.Q., Lyu, Z., Ma, B., 2019b. Convergent continental margin volcanic source for ash beds at the Permian–Triassic boundary, South China: Constraints from trace elements and Hf isotopes. Palaeogeogr. Palaeoclimatol. Palaeoecol (In this volume).
Wignall, P.B., Sun, Y.D., Bond, D.P.G., Izon, G., Newton, R.J., Védrine, S., Widdowson, M., Ali, J.R., Lai, X.L., Jiang, H.S., Cope, H., Bottrell, S.H., 2009. Volcanism, mass extinction and carbon isotope fluctuations in the Middle Permian of China. Science 324, 1179–1182.
Wu, S., Chen, Z.Q., Fang, Y., Pei, Y., Yang, H., Ogg, J., 2017. A Permian–Triassic boundary microbialite deposit from the eastern Yangtze Platform (Jiangxi Province, South China): geobiologic features, ecosystem composition and redox conditions. Palaeogeogr. Palaeoclimatol. Palaeoecol. 486, 58–73.
Xie, S., Pancost, R.D., Yin, H., Wang, H., Evershed, R.P., 2005. Two episodes of microbial change coupled with Permo/Triassic faunal mass extinction. Nature 434, 494–497.
Xie, S., Pancost, R.D., Wang, Y., Yang, H., Wignall, P.B., Luo, G., Jia, C., Chen, L., 2010. Cyanobacterial blooms tied to volcanism during the 5 myr Permo–Triassic biotic crisis. Geology 38, 447–450.
Xu, Y., Chen, Z.Q., Feng, X., Wu, S., Shi, G.R., Tu, C., 2017. Proliferation of MISS-related microbial mats following the end-Permian mass extinction in the northern Paleo-Tethys: evidence from southern Qilianshan region, western China. Palaeogeogr. Palaeoclimatol. Palaeoecol. 474, 198–213.
Yang, Z., Wu, S., Yin, H.F., Xu, G., Zhang, K., 1991. Geological Events during Permian and Triassic Transition in South China. Geological Publishing House, Beijing, pp. 35–63 (in Chinese).
Yang, H., Chen, Z.Q., Kershaw, S., Liao, W., Lü, E.L., Huang, Y., 2019. Small microbialites from the basal Triassic mudstone (Tieshikou, Jiangxi, South China): geobiologic features, biogenicity, and paleoenvironmental implications. Palaeogeogr. Palaeoclimatol. Palaeoecol (In this volume).
Yin, H.F., Huang, S., Zhang, K.X., Hansen, H.J., Yang, F.Q., Ding, M., Bie, X.M., Sweet, W.C., 1992. The effects of volcanism on the Permo–Triassic mass extinction in South China. In: Sweet, W.C., Yang, Z., Dickins, J.M., Yin, H.F. (Eds.), Permo–Triassic Events in the Eastern Tethys. Cambridge University Press, Cambridge, pp. 146–157.
Yin, H.F., Feng, Q., Lai, X., Baud, A., Tong, J., 2007. The protected Permo–Triassic crisis and multi-episode extinctions around the Permian–Triassic boundary. Glob. Planet. Chang. 55, 1–20.
Yu, J., Broutin, J., Chen, Z.Q., Shi, X., Li, H., Chu, D., Huang, Q., 2015. Vegetation changeover across the Permian − Triassic boundary in southwest China: extinction, survival, recovery and paleoclimate: a critical review. Earth-Sci. Rev. 149, 203–224.
Zhang, G., Zhang, X., Li, D., Farquhar, J., Shen, S., Chen, X., Shen, Y.A., 2015. Widespread shoaling of sulfidic waters linked to the end-Guadalupian (Permian) mass extinction. Geology 43, 1091–1094.
Zhang, F.F., Algeo, T.J., Romaniello, S.J., Cui, Y., Zhao, L., Chen, Z.Q., Anbar, A.D., 2018. Congruent Permian–Triassic δ^{238}U records at Panthalassic and Tethyan sites: confirmation of global-oceanic anoxia and validation of the U-isotope paleoredox proxy. Geology 46, 327–330.
Zhang, L., Orchard, M.J., Algeo, T.J., Chen, Z.Q., Lyu, Z., Zhao, L., Kaiho, K., Ma, B., Liu, S., 2019. An intercalibrated Triassic conodont succession and carbonate carbon isotope profile, Kamura, Japan. Palaeogeogr. Palaeoclimatol. Palaeoecol (In this volume).
Zhao, L., Orchard, M.J., Tong, J., Sun, Z., Zuo, J., Zhang, S., Yun, A., 2007. Lower Triassic conodont sequence in Chaohu, Anhui Province, China and its global correlation. Palaeogeogr. Palaeoclimatol. Palaeoecol. 252, 24–38.
Zhao, L., Chen, Y., Chen, Z.Q., Cao, L., 2013a. Uppermost Permian to Lower Triassic conodont zonation from Three Gorges area, South China. Palaios 28, 523–540.
Zhao, L., Chen, Z.Q., Algeo, T.J., Chen, J., Chen, Y., Tong, J., Gao, S., Zhou, L., Hu, Z., Liu, Y., 2013b. Rare-earth element patterns in conodont albid crowns: evidence for massive inputs of volcanic ash during the latest Permian biocrisis? Glob. Planet. Chang. 105, 135–151.
Zhao, X., Tong, J., Yao, H., Niu, Z., Luo, M., Huang, Y., Song, H., 2015. Early Triassic trace fossils from the Three Gorges area of South China: implications for the recovery of benthic ecosystems following the Permian–Triassic extinction. Palaeogeogr. Palaeoclimatol. Palaeoecol. 429, 100–116.

Zhong-Qiang Chen[a,*], Thomas J. Algeo[a,b,c], Shane D. Schoepfer[d]
[a] *State Key Laboratory of Biogeology and Environmental Geology, China University of Geosciences (Wuhan), Wuhan 430074, China*
[b] *Department of Geology, University of Cincinnati, Cincinnati, OH 45221-0013, USA*
[c] *State Key Laboratory of Geological Processes and Mineral Resources, China University of Geosciences (Wuhan), Wuhan 430074, China*
[d] *Department of Geoscience, University of Calgary, Calgary, Alberta T2N 1N4, Canada*
E-mail addresses: zhong.qiang.chen@cug.edu.cn (Z.-Q. Chen), Thomas.Algeo@uc.edu (T.J. Algeo), shane.schoepfer@ucalgary.ca (S.D. Schoepfer).

[*] Corresponding author.